FURTHER EVIDENCE FOR JET STRUCTURE IN LARGE $p_\perp$ REACTIONS FROM RAPIDITY CORRELATIONS AND ASSOCIATED MULTIPLICITIES

By J. Ranft and Gisela Ranft

Sektion Physik, Karl-Marx-Universität, Leipzig*

(Received November 23, 1976)

Using the hard collision model and a simple parametrisation for jet fragmentation we derive expressions for same side and opposite side two-particle correlations and multiplicities associated with large transverse momentum trigger particles. Recent data on rapidity correlations and associated multiplicities can be well understood in such a model. We interpret this result as further evidence for the presence of jets in large transverse momentum reactions.

1. Introduction

There was considerable progress in the understanding of collision processes with large transverse momentum particles within the last year [1, 2].

In this paper we use the hard collision model [3] which we did use before in Ref. [4] — which in the following is denoted by I — for the calculation of inclusive cross sections for the production of one or several particles. In I and in a similar way in Refs [5] to [9] transverse momentum correlations at $\Theta \approx 90°$ were worked out as function of transverse momentum. The emphasis of the present paper is on correlations of large transverse momentum particles in the rapidity variable and on associated multiplicities. As in [10] we consider jet fragmentation functions where the transverse momenta of particles relative to the jet axis are taken into account, the parametrisation proposed in the present paper has however practical advantages against the one used in Ref. [10]. We use jet production cross sections according to the hard collision model which were found in Ref. [11] to describe known data on opposite side rapidity correlations and the rapidity dependence of single particle spectra at large $q_\perp$.

The paper is organized as follows: In Section 2 and Appendix A we describe inclusive jet fragmentation functions and jet fragmentation multiplicities. In Section 3 and Appendix B we calculate inclusive distributions of one or several particles in large $q_\perp$ reactions. The

*Address: Sektion Physik, Karl-Marx-Universität, Linnestrasse 5, 701 Leipzig, DDR.

resulting expressions are compared with data on the Δy distributions of two particles on the same and on the opposite side. These data [12, 13] give the best presently available evidence for the appearance of jets in large $q_\perp$ reactions. In Section 4 we calculate same side and opposite side associated multiplicities and compare with experimental data.

2. *Production and fragmentation of jets*

2.1. Jet fragmentation

In papers I and II Ref. [10] we considered in detail a parametrisation for the jet fragmentation in the jet frame. We used as variables the longitudinal momentum $p_\parallel$ along the jet axis and the transverse momentum $p_\perp$ perpendicular to this axis,

$$\mathscr{E}\frac{d^3n}{d^3p} \sim \frac{F+1}{\pi b^2}\left(1-\frac{p_\parallel}{P}\right)^F e^{-\frac{p_\perp^2}{b^2}}. \tag{2.1}$$

Inclusive one-, two-, and three-particle distributions at large transverse momentum $q_\perp$ taking the transverse momentum distribution within the jet into account were calculated in II. Due to the considerable number of integrations, the resulting expressions were rather cumbersome and numerical evaluation of multiple integrals was necessary to obtain distributions which are of interest for phenomenological applications.

In order to calculate the inclusive distributions of interest more elegantly we propose here an approximate jet fragmentation function parametrized in the variables of the overall c.m.s. In particular we use the rapidity y, transverse momentum $q_\perp$, and azimuthal angle φ of the observed hadron and the rapidity Y_J, transverse momentum $P_\perp$, azimuthal angle Φ_J of the jet in the total c.m.s. Furthermore we use variables in the parton-parton c.m.s. which are denoted by a hat, such as the total jet energy $\hat{E}_J = \sqrt{\hat{s}}/2$, the jet rapidity $\hat{Y}_J$, and the polar angle $\hat{\Theta}_J$. These are related by

$$\cosh \hat{Y}_J = \frac{\hat{E}_J}{P_\perp} = \frac{1}{\sin \hat{\Theta}_J}. \tag{2.2}$$

The invariant mass of the jet is $M_J \approx 0$. In these variables our approximate jet fragmentation functions is

$$\frac{d^3n(\hat{s})}{dy d\varphi q_\perp dq_\perp} = \mathscr{A}\left(\frac{\sqrt{\hat{s}}}{2}\right)\frac{F+1}{q_\perp^2}\left(1-\frac{q_\perp}{P_\perp}\right)^F \frac{1}{\sqrt{\pi}\,c}\exp\left[-\frac{(\varphi-\Phi_J)^2}{c^2}\right]$$

$$\times \frac{1}{\sqrt{\pi}\,c}\exp\left[-\frac{(y-Y_J)^2}{c^2}\right] \tag{2.3}$$

with

$$c = \frac{b}{q_\perp}. \tag{2.4}$$

The parameter b characterizes the transverse momentum dependence in (2.1). The Gaussians are convenient for integrations. The widths of the Gaussians in rapidity is motivated by the calculations in II. The shape of the φ distribution follows from (2.1) by approximating $\sin^2(\varphi-\Phi_J) \approx (\varphi-\Phi_J)^2$. The normalisation can be determined from the energy sum rule; asymptotically it is

$$\mathscr{A}\left(\frac{\sqrt{\hat{s}}}{2}\right) \sim 1. \tag{2.5}$$

Integrating the distribution (2.3) over the whole interval in y, φ, and $q_\perp$ we obtain the multiplicity of hadrons per jet $\langle n\rangle_J$,

$$\begin{aligned}\langle n\rangle_J &= \int \frac{d^3n(\hat{s})}{dy d\varphi q_\perp dq_\perp} dy d\varphi q_\perp dq_\perp \\ &= \mathscr{A}\left(\frac{\sqrt{\hat{s}}}{2}\right)(F+1) \int_{b'/\cosh \hat{Y}_J}^{P_+} q_\perp dq_\perp \frac{1}{q_\perp^2}\left(1-\frac{q_\perp}{P_\perp}\right)^F \\ &\times \int_{\hat{Y}_J-\Delta}^{\hat{Y}_J+\Delta} dy \int_{\Phi_J-\pi/2}^{\Phi_J+\pi/2} d\varphi \frac{1}{c\sqrt{\pi}} \exp\left[-\frac{(\varphi-\Phi_J)^2}{c^2}\right] \frac{1}{\sqrt{\pi}\, c} \exp\left[-\frac{(y-Y_J)^2}{c^2}\right].\end{aligned} \tag{2.6}$$

The transverse momentum $q_\perp$ varies in the range

$$\frac{b'}{\cosh \hat{Y}_J} < q_\perp < P_\perp; \quad P_\perp = \frac{\hat{E}_J}{\cosh \hat{Y}_J}; \quad \hat{E}_J = \frac{\sqrt{\hat{s}}}{2}, \tag{2.7}$$

where b' is a low momentum cut-off in the jet system. Further, Δ appearing in the y — integration limits is used as

$$\Delta = \cosh^{-1} \frac{\hat{E}_J}{\sqrt{q_{\perp 2}^2+m^2}} - \hat{Y}_J = \Delta(q_{\perp 2}) \tag{2.8}$$

with the particle mass m. The approximate integration, extending the integration limits in y and φ to infinity, yields for $F = 1$ or 2

$$\langle n\rangle_J = (F+1)\left[\ln \frac{\hat{E}_J}{b'} - F\left(1-\frac{b'}{\hat{E}_J}\right) + \tfrac{1}{2}(F-1)\left(1-\frac{b'^2}{\hat{E}_J^2}\right)\right]. \tag{2.9}$$

In Appendix A we define analogously the inclusive two-particle distribution from the jet fragmentation.

2.2. Jet production

According to the hard collision model [3, 14], the cross section for production of two jets has the form

$$\frac{d^4\sigma_J(s)}{dP_\perp dY_s dY_0 d\Phi} = \frac{1}{\pi} P_\perp^2 \sum_{i,j} f_{iA}(x_1) f_{jB}(x_2) \frac{d\hat{\sigma}_{ij}}{d\hat{t}}. \tag{2.10}$$

The indices s and o denote variables of the same side and opposite side jets. Due to transverse momentum conservation it is

$$P_{\perp s} = P_{\perp o} = P_\perp \tag{2.11}$$

and

$$\Phi_s = \Phi, \quad \Phi_0 = \Phi + \pi.$$

The function $\frac{1}{x_1} f_{iA}(x_1) \left[\frac{1}{x_2} f_{jB}(x_2)\right]$ gives the probabilities to find the parton i [j] in the hadron A [B] with the momentum fraction $x_1 = p_i/P_A$ [$x_2 = p_j/P_B$].

$d\sigma_{ij}/d\hat{t}$ is the parton-parton scattering cross section; $\hat{t}$ and $\hat{s}$ refer to the parton-parton collision. The following kinematic relations apply [3]

$$\begin{aligned} \eta &= \operatorname{tg}\frac{\Theta_s}{2}\operatorname{ctg}\frac{\Theta_o}{2} & x_1 &\approx \frac{P_\perp}{\sqrt{s}}\left(\operatorname{ctg}\frac{\Theta_s}{2} + \operatorname{ctg}\frac{\Theta_o}{2}\right) \\ \hat{s} &= P_\perp^2(1+\eta)\left(1+\frac{1}{\eta}\right) & x_2 &\approx \frac{P_\perp}{\sqrt{s}}\left(\operatorname{tg}\frac{\Theta_s}{2} + \operatorname{tg}\frac{\Theta_o}{2}\right) \\ \hat{t} &= -P_\perp^2(1+\eta) \end{aligned} \tag{2.12}$$

For $d\sigma_{ij}/d\hat{t}$ we use a parametrization which was found in [11] to describe opposite side rapidity distributions

$$\frac{d\sigma_{ij}}{d\hat{t}} = \frac{1}{\hat{s}^n}\left(a + \eta + \frac{1}{\eta}\right)^l \tag{2.13}$$

with $a = 0.5$, $l = 3$ for the hard scattering process $qM \to qM$ and $a = 1$, $l = 3$ for $qq \to$ jet + jet. n has to be chosen such that the $q_\perp$ dependence of single particle distributions agrees with experiment ($n \approx 4$).

We use Eqs (2.10) and (2.13) for calculating the same side and opposite side associated multiplicities in their $q_{\perp 1}$, y_1 dependence. For calculating the rapidity correlations of two particles on the trigger side or on the opposite side we use the following simple approximation for the two-jet distribution

$$\frac{d^4\sigma_J(s)}{dY_s dY_o dP_\perp d\Phi} = C\frac{1}{P_\perp^N}\exp\left(-\frac{2DP_\perp}{\sqrt{s}}\right)\frac{1}{\sqrt{2\pi}\,B_s}e^{-\frac{Y_s^2}{2B_s^2}}\frac{1}{\sqrt{2\pi}\,B_o}e^{-\frac{Y_o^2}{2B_o^2}}. \tag{2.14}$$

Here the same side and opposite side jet rapidities Y_s and Y_o are uncorrelated. This uncorrelated ansatz and the Gaussian shape of the rapidity distributions is motivated by the experimental observation [13, 15] for present trigger transverse momenta ($x_\perp = P_\perp/\sqrt{s}/2 \simeq 0.1$). As shown in [11], the two-jet distribution (2.10) with Eq. (2.13) has for these $x_\perp$ values of the trigger exactly this uncorrelated property. We should however keep in mind that Y_s, Y_o correlations appear for larger trigger momenta [11].

3. *Jet structure in same and opposite side rapidity distributions*

In Appendix B we collect expressions for inclusive distributions at large transverse momentum. These expressions are derived using the uncorrelated expression for the two-jet production cross section (2.14) and the jet fragmentation functions (2.3) and (A.1). It is the advantage of our parametrisation that the complicated integral expressions factorize and that most of the integral terms can be evaluated analytically. We should keep in mind that the uncorrelated expression for the two-jet production cross section is only justified for small $x_\perp$ of the trigger particle like in presently available experiments from the CERN-SFM [12] as discussed already in Section 2. Our expressions should be valid more generally if, e.g., the rapidity distribution of two particles, both on the same or on the opposite side, is considered.

The transverse momentum dependence of the single particle distribution (B.2) and the same side and opposite side two-particle distributions (B.7) and (B.13) can be used to study questions like trigger bias and same side and opposite side large transverse momentum correlations. This was done in I as well as in Refs [3] and [6]. The $q_\perp$ dependence of the expressions in Appendix B is the same as found in I; therefore we shall not discuss these matters in detail here.

Two particles emitted from the same side jet are characterized by the distribution in their rapidity difference, see (B.7), which is of the form

$$W_2((y_1-y_2), B_s, c_1, c_2) = \frac{1}{\sqrt{\pi}\sqrt{\dfrac{c_1^2c_2^2}{2B_s^2}+c_1^2+c_2^2}} \exp\left[-\frac{(y_1-y_2)^2}{\dfrac{c_1^2c_2^2}{2B_s^2}+c_1^2+c_2^2}\right]. \tag{3.1}$$

The characteristic correlation length is

$$\begin{aligned} L(q_{\perp 1}, q_{\perp 2}) &= \frac{1}{\sqrt{2}}\sqrt{\frac{c_1^2c_2^2}{2B_s^2}+c_1^2+c_2^2} \\ &= \frac{b}{\sqrt{2}\,q_{\perp 1}q_{\perp 2}}\sqrt{\frac{b^2}{2B_s^2}+q_{\perp 1}^2+q_{\perp 2}^2}\,. \end{aligned} \tag{3.2}$$

$L(q_{\perp 1}, q_{\perp 2})$ decreases with rising transverse momenta of one or both particles. For large $q_{\perp 1}$ the constant term $b^2/2B_s^2$ can be neglected and we obtain the limiting behaviour

$$L(q_{\perp 1}, q_{\perp 2}) = \begin{cases} \dfrac{b}{\sqrt{2}\,q_{\perp 2}} & \text{for } q_{\perp 1} \gg q_{\perp 2}, \\ \dfrac{b}{\sqrt{2}\,q_{\perp 1}} & \text{for } q_{\perp 2} \gg q_{\perp 1}. \end{cases} \tag{3.3}$$

This behaviour of the correlation length was already obtained as an approximation in a more complicated way in II. In Table 3.1 we compare the calculated correlation lengths with experimental values which we read off the experimental distributions given by Darriulat et al. [12]. Calculated and experimental correlation lengths agree rather well. Before

TABLE 3.1

Comparison of the experimental [12] and theoretical correlation length in the same side two-particle rapidity distribution, Eq. (3.2). It is $q_{\perp 1} = 2$ GeV/c. Further $b = 0.355$ (GeV/c)$^{-1}$, see I

$q_{\perp 2}$ (GeV/c)	$L(q_{\perp 1}, q_{\perp 2})$	L_{exp}	Range of experimental $q_\perp$ interval
0.5	0.52	0.66	0.4 — 0.6
0.7	0.38	0.58	0.6 — 0.8
0.9	0.31	0.50	0.8 — 1.1
1.2	0.24	0.33	1.1 — 1.7

interpreting this results as evidence for same side jets, however, a more careful study of two- and three-body resonances is necessary.

Rapidity correlations of transverse momentum analyzed particles opposite to a trigger particle were recently measured by the CCHK collaboration [12]. This data gives evidence for the opposite side jet. In the following we analyse this data using our method. According to Eq. (B.14) the distribution in rapidity difference for two opposite side particles has the same form as Eq. (3.2). The CCHK collaboration determines the normalised distribution

TABLE 3.2

The azimuthal acceptance functions $A_1(\Delta\phi, c_1, c_2)$ and $A_2(\Delta\phi, c_1, c_2, c_3)$ Eqs (B.9) and (B.15) for $q_{\perp 1} = 2.5$ GeV/c as function of transverse momenta and $\Delta\phi$

a) $A_1(\Delta\phi, c_1, c_2)$

$q_{\perp 2}$ \ $\Delta\phi$	9°	27°	45°	63°	81°
0.2	0.10	0.30	0.48	0.63	0.75
0.6	0.29	0.74	0.94	0.991	0.999
1.0	0.45	0.93	0.997	~1.	~1.
1.4	0.57	0.98	~1.	~1.	~1.
1.8	0.65	0.995	~1.	~1.	~1.

b) $A_2(\Delta\phi, c_1, c_2, c_3)$

$q_{\perp 2} = q_{\perp 3}$ \ $\Delta\phi$	9°	27°	45°	63°	81°
0.2	0.01	0.09	0.23	0.40	0.56
0.6	0.08	0.54	0.88	0.98	0.998
1.0	0.20	0.86	0.99	~1.	~1.
1.4	0.33	0.96	~1.	~1.	~1.
1.8	0.44	0.99	~1.	~1.	~1.

$dN^c/d(y_2-y_3)$ of two opposite side particles and a corresponding normalised uncorrelated distribution $dN^{unc}/d(y_2-y_3)$ which is obtained by combining particles from different events. Using these two distributions the divided correlation $R(\Delta y)$ is determined

$$R(\Delta y) = \frac{dN^c}{d(y_2-y_3)} \Big/ \frac{dN^{unc}}{d(y_2-y_3)} . \tag{3.4}$$

The data is given for trigger momenta $q_{\perp 1} \simeq 2.5$ GeV/c and transverse momenta on the opposite side in three ranges $q_{\perp 2}$ and $q_{\perp 3} \geqslant 0.3$, 0.6 and 0.9 GeV/$c$. These distributions are reproduced in our Figures 3.1, 3.2 and 3.3. It should be noted that the experimental distributions at small Δy are distorted by a reduced efficiency for detecting closeby tracks[10].

In our calculation, the uncorrelated distribution of two opposite side particles can be deduced from Eq. (B.8). It has the form

$$\frac{dN^{unc}}{d(y_2-y_3)} = \frac{1}{\sqrt{\pi}\sqrt{4B_0^2+c_2^2+c_3^2}} \exp\left[-\frac{(y_2-y_3)^2}{4B_0^2+c_2^2+c_3^2}\right]. \tag{3.5}$$

In comparing our distribution with experiment we have to take into account that the azimuthal acceptances $A_1(\Delta\Phi, c_1, c_2)$ and $A_2(\Delta\Phi, c_1, c_2, c_3)$, Eqs. (B.9) and (B.15), for detecting one or two particles from the opposite side jet are different. In Table 3.2 we give values for these acceptance functions calculated from (B.9) and (B.15). As to be expected, the acceptance $A_2(\Delta\Phi, c_1, c_2, c_3)$ for detecting two particles in a given range $\Delta\Phi$ is smaller than $A_1(\Delta\Phi, c_1, c_2)$. In the comparison we take further into account that not all particles detected on the opposite side result from the hard collision process. We use a two component model for the inclusive distribution N

$$N = \alpha N^{\text{hard coll.}} + (1-\alpha) N^{\text{low } q_\perp \text{ background}} \tag{3.6}$$

We treat α as a free parameter.

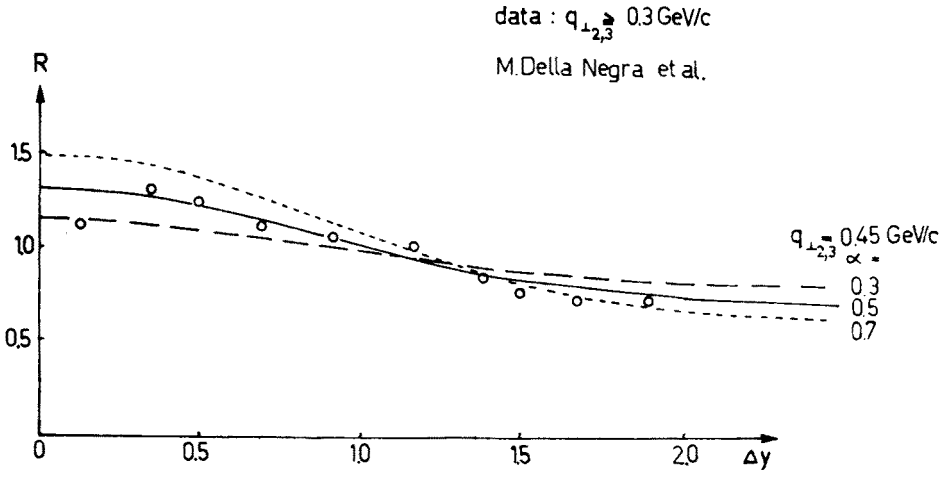

Fig. 3.1. The ratio $R(\Delta y)$ (Eq. (3.4)) as function of Δy for various values of the parameter α, $\alpha = 0.3$, 0.5 and 0.7 at $q_{\perp 2} = q_{\perp 3} = 0.45$ GeV/c compared with data of Ref. [13] for $q_{\perp 2}$ and $q_{\perp 3} \geqslant 0.3$ GeV/c. The data for $\Delta y \lesssim 0.5$ are strongly biased by limited acceptance

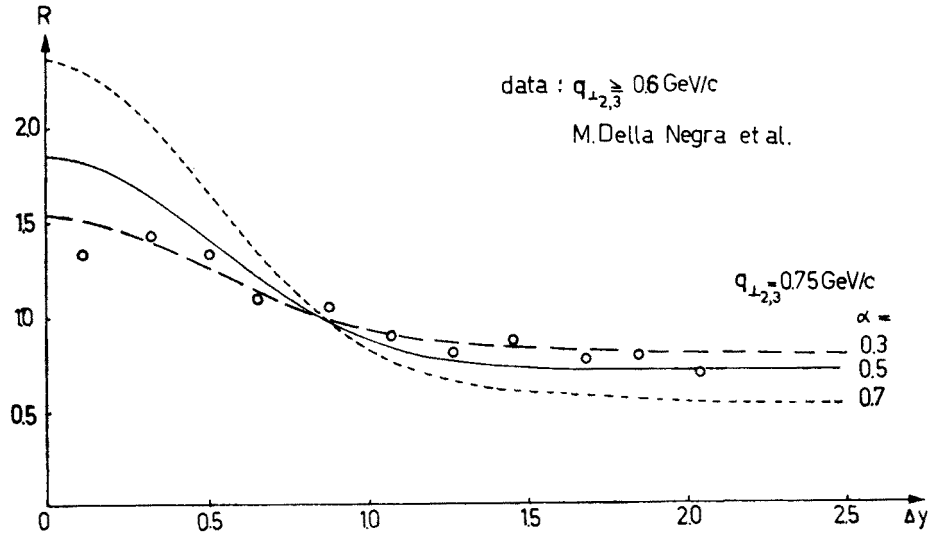

Fig. 3.2. The ratio $R(\Delta y)$ as in Figure 3.1; the theoretical curves are for $q_{\perp 2} = q_{\perp 3} = 0.75$ GeV/c, the experimental data are for $q_{\perp 2}$ and $q_{\perp 3} \geqslant 0.6$ GeV/c

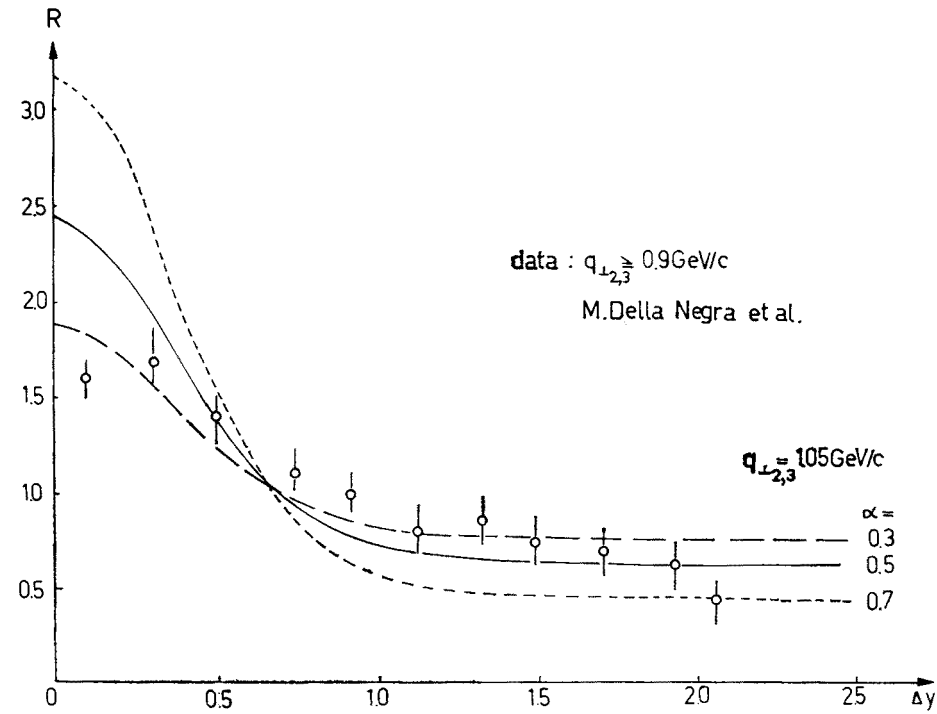

Fig. 3.3. The ratio $R(\Delta y)$ as in Figure 3.1; the theoretical curves are for $q_{\perp 2} = q_{\perp 3} = 1.05$ GeV/c, the experimental data are for $q_{\perp 2}$ and $q_{\perp 3} \geqslant 0.9$ GeV/c

In Figures 3.1, 3.2 and 3.3 we compare the data for oppositely charged particles with the result of our calculation. The calculation is for fixed average values of the transverse momenta as given on the plots. For reasonable α values around 0.5 the calculated curves agree well with the data outside the region $\Delta y \simeq 0$. The width of the peak at low Δy decreases with rising $q_{\perp_1}$ and $q_{\perp_2}$ as in the data. This agreement can be interpreted as evidence of jets on the opposite side.

4. Associated multiplicities

4.1. Associated multiplicities in the hard collision model

In this Section we calculate multiplicities associated to one large transverse momentum trigger particle. The trigger particle is characterized by the transverse momentum $q_{\perp_1}$ and the rapidity y_1 and we compute the number of associated particles at rapidity y_2 integrated over all transverse momenta $q_{\perp_2}$ within a given acceptance in the azimuthal angle φ on the same side or the opposite side to the trigger particle. We study in detail these associated multiplicities in a hard collision model considering the particles from the two jets. Associated multiplicities were recently studied by Abad et al. [16]. They study in detail the associated multiplicities from low $q_\perp$ background and use for the large $q_\perp$ component only the relation

$$\langle n \rangle_J \sim \langle P_\perp \rangle, \tag{4.1}$$

i.e. fragmentation multiplicity from one jet proportional to average jet transverse momentum. We shall not consider the low $q_\perp$ background again, but we treat the multiplicities due to the large $P_\perp$ jets in a more detailed way consistent with the jet fragmentation functions used elsewhere in this paper. There are two possibilities to calculate the multiplicities of jets in large $q_\perp$ reactions

(*i*) jets are considered in the c.m.s. of the irreducible subcollision of two partons. These jets are characterized by the energy $\sqrt{\hat{s}}/2$ and by jet multiplicities as calculated in Section 2, Eq. (2.9) and in Appendix A, Eq. (A.4).

(*ii*) jets are considered in the total c.m.s. of the collision. Then the jet energy differs from $\sqrt{\hat{s}}/2$ and therefore the jet multplicity is different from the one in case (*i*).

Here we adopt the possibility (*i*) where the total multiplicity of the two jets agrees with the multiplicity observed in $e^+ e^-$ annihilation if quark-like jets are considered.

After these preliminaries we give the expressions for same side and opposite side associated multiplicities (two-jet component only). We discuss first the opposite side multiplicity which is more simple. We start from the basic formula (B.11) for the distribution of one trigger particle and one particle on the opposite side. To calculate the multiplicity from the opposite side jet we replace the opposite side jet fragmentation function under the integral by the expression for the jet multiplicity (2.9). The integrals over $d\varphi_2$ and $d\Phi$ in the resulting expression factorize if we replace $q_{\perp_2}$ by its average value in the terms containing the azimuthal angle. Then they lead to the azimuthal acceptance function $A_1(\Delta\Phi, c_1, c_2 = b/\langle q_{\perp_2} \rangle)$ defined in (B.9). To obtain the associated multiplicity we have

to divide finally by the distribution of the trigger particle

$$\langle n_2(s, y_2; q_{\perp 1}, y_1, \varphi_1 = 0; \Delta\Phi\rangle_{\text{opp}}$$

$$= \frac{A_1\left(\Delta\Phi, c_1, \dfrac{b}{\langle q_{\perp 2}\rangle}\right) \displaystyle\int_{q_{\perp 1}}^{\sqrt{s}/2} dP_\perp \int_{Y_{o1}}^{Y_{o2}} dY_o \int_{Y_{s1}}^{Y_{s2}} dY_s \frac{d^3\sigma_J}{dY_s dY_o dP_\perp} \frac{d^3 n_s(\hat{s})}{dq_{\perp 1} dy_1 d\varphi_1}\Big|_{\varphi_1=0} \langle \bar{n}_o(\hat{s}, y_2)\rangle_J}{\displaystyle\int_{q_{\perp 1}}^{\sqrt{s}/2} dP_\perp \int_{Y_{s1}}^{Y_{s2}} dY_s \int_{Y_{o1}}^{Y_{o2}} dY_o \frac{d^3\sigma_J}{dY_s dY_o dP_\perp} \frac{d^3 n(\hat{s})}{dq_{\perp 1} dy_1 d\varphi_1}\Big|_{\varphi_1=0}}, \tag{4.2}$$

where we have defined

$$\langle \bar{n}_o(\hat{s}, y_2)\rangle_J = \langle n_o(\hat{s})\rangle \frac{1}{\sqrt{\pi}\dfrac{b}{\langle q_{\perp 2}\rangle}} \exp\left[-\frac{(y_2 - Y_o)^2}{(b/\langle q_{\perp 2}\rangle)^2}\right]. \tag{4.3}$$

In the denominator we have performed the integral over $d\Phi$; it gives approximately 1 for large $q_{\perp 1}$. For the jet multiplicity $\langle \bar{n}_o(\hat{s}, y_2)\rangle_J$ we insert the expression (2.9); for the jet fragmentation functions we use Eq. (2.3) integrated over Φ_J; for the jet production function we insert the hard collision expression (2.10). In Ref. [11] it was shown that presently known data on opposite side rapidity correlations can be described by subprocesses like q+q → q+q or q+M → q+M (q = quark, M = meson) if the cross section $d\sigma_{ij}/d\hat{t}$ is suitably chosen. Here we use the results of Ref. [11] but restrict ourselves to the subprocess q+q → q+q → jet+jet. We use the quark distribution functions $f_{iA}(x)$ according to the fit of Barger and Phillips [17] and adopt for $d\sigma_{ij}/d\hat{t}$ the empirical parametrisation from Kripfganz and Ranft [11],

$$\frac{d\sigma_{ij}}{d\hat{t}} \sim \frac{1}{\hat{s}^4} f(\eta), \quad f(\eta) = \left(1 + \eta + \frac{1}{\eta}\right)^3. \tag{4.4}$$

η, $\hat{s}$ and other kinematical quantities are defined in (2.12). With the integrands described, the nominator and denominator of (4.2) have to be evaluated numerically.

For the same side associated multiplicities we use similar approximations and describe jet production and fragmentation as above. The resulting expression for the same side associated multiplicity is

$$\langle n_2(s, y_2, q_{\perp 1}, y_1, \varphi_1 = 0; \Delta\Phi\rangle_{\text{same}}$$

$$= A_1\left(\Delta\Phi, c_1, c_2 = \frac{b}{\langle q_{\perp 2}\rangle}\right) \int_{q_{\perp 1}}^{\sqrt{s}/2} dP_\perp \int_{Y_{o1}}^{Y_{o2}} dY_o \int_{Y_{s1}}^{Y_{s2}} dY_s \frac{d^3\sigma_J}{dY_s dY_o dP_\perp} \times \left\{\frac{d^3 n_s(\hat{s})}{dq_{\perp 1} dy_1 d\varphi_1}\Big|_{\varphi_1=0} \langle \bar{n}_s(\hat{s}, y_2)\rangle_J\right\}$$

$$= \frac{\displaystyle\int_{q_{\perp 1}}^{\sqrt{s}/2} dP_\perp \int_{Y_{s1}}^{Y_{s2}} dY_s \int_{Y_{o1}}^{Y_{o2}} dY_o \frac{d^3\sigma_J}{dY_s dY_o dP_\perp} \frac{d^3 n(\hat{s})}{dq_{\perp 1} dy_1 d\varphi_1}\Big|_{\varphi_1=0}}{\displaystyle\int_{q_{\perp 1}}^{\sqrt{s}/2} dP_\perp \int_{Y_{s1}}^{Y_{s2}} dY_s \int_{Y_{o1}}^{Y_{o2}} dY_o \frac{d^3\sigma_J}{dY_s dY_o dP_\perp} \frac{d^3 n(\hat{s})}{dq_{\perp 1} dy_1 d\varphi_1}\Big|_{\varphi_1=0}}. \tag{4.5}$$

The expression in the curly brackets is defined in Eq. (A.4). The intgrals in (4.5) are again evaluated numerically.

In Fig. 4.1 we plot the same side and opposite side associated multiplicities (4.2) and (4.5) for $y_1 = y_2 = 0$ as function of the trigger transverse momentum $q_{\perp_1}$ for 3 values of $\sqrt{s}$. The same side associated multiplicity is small and independent of the trigger

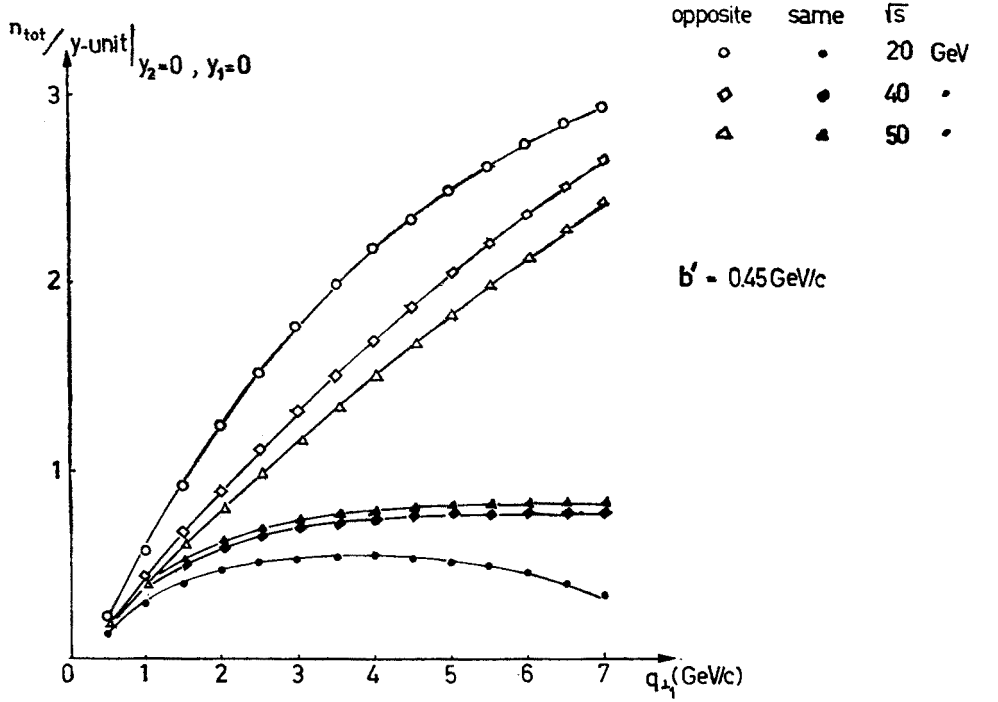

Fig. 4.1. Theoretical curves of the same side and opposite side multiplicity per rapidity unit at $y_2 = y_1 = 0$ as function of trigger transverse momentum $q_{\perp_1}$, Eqs (4.2) and (4.5), for $\sqrt{s} = 20$, 40 and 50 GeV/c. The parameter b' is $b' = 0.45$ GeV/c (all hadrons)

transverse momentum; the opposite side associated multiplicity rises in the $q_{\perp_1}$ range presently of interest approximately linearly with $q_{\perp_1}$. This result justifies the ansatz (4.1) of Abad et al. [16].

4.2. Comparison with data

In our comparison with data on associated multiplicities at large transverse momentum we are mainly interested in the overall consistency of the hard collision model. Therefore we try to understand the associated multiplicities due to the hard collision process in their absolute size and in their dependence on the trigger transverse momentum and on rapidity. We adopt the approach used by experimental groups (e.g. by Kephart et al. [18]) that the associated multiplicity due to the large $q_\perp$ process is equal to the total observed associated multiplicity minus the multiplicity of the background low $q_\perp$ component which is assumed to be equal to the multiplicity in a normal event at the c.m.s. energy correspon-

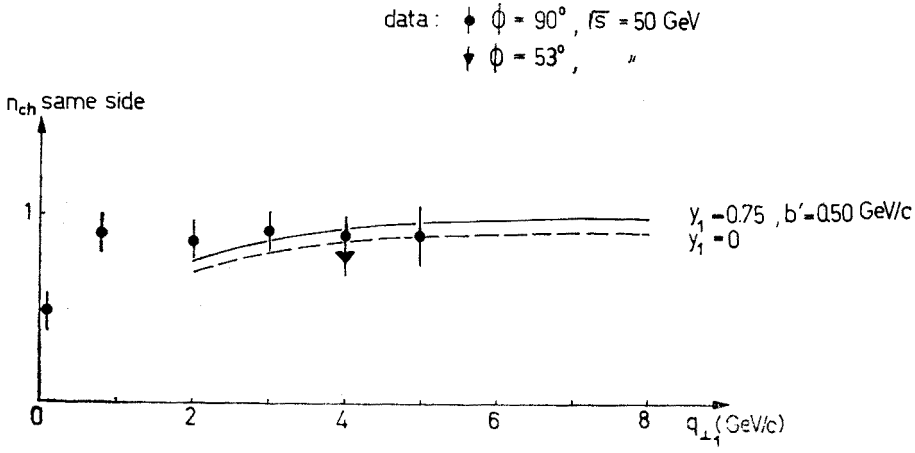

Fig. 4.2. The same side charged multiplicity as function of the trigger transverse momentum $q_{\perp 1}$ for trigger rapidity $y_1 = 0$ and $y_1 = 0.75$ and parameter $b' = 0.50$ GeV/c, compared with data of Ref. [1] at $\sqrt{s} = 50$ GeV and at angles $\phi = 90°$ and $\phi = 53°$

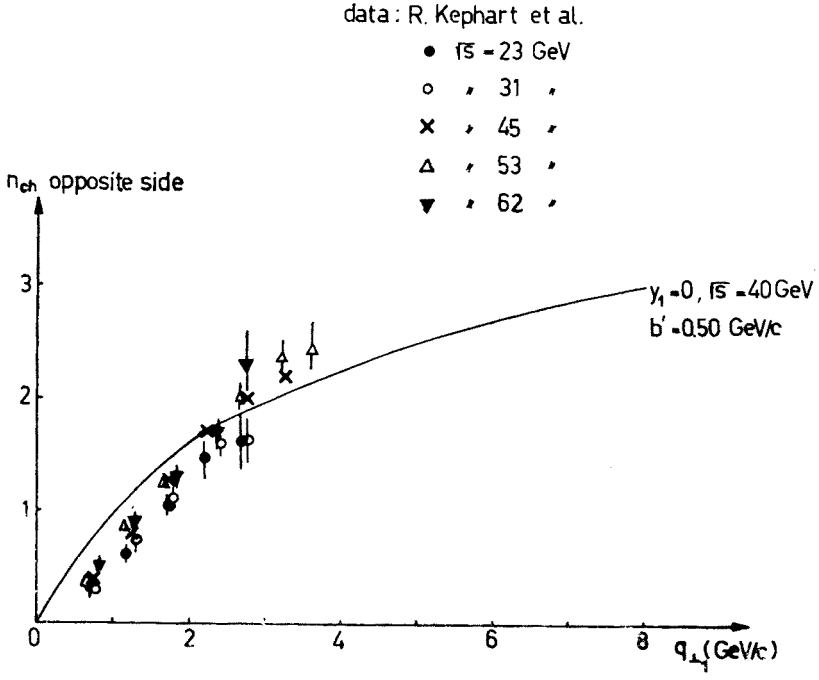

Fig. 4.3. The opposite side charged multiplicity at trigger rapidity $y_1 = 0$ as function of trigger transverse momentum $q_{\perp 1}$, computed for $\sqrt{s} = 40$ GeV and the parameter $b' = 0.50$ GeV/c, and compared with data of Ref. [18] at $23 \leqslant \sqrt{s} \leqslant 62$ GeV

ding to the actual c.m.s. energy minus energy of the two jets. We compare the associated multiplicity due to the hard collision process as calculated above directly with experimental data obtained using this approach. As indicated above we shall not repeat here an analysis like the one of Abad et al. [16].

When calculating associated multiplicities, we introduce only one new parameter, the low momentum cut-off b' in Eq. (2.6). We find best agreement to all data using $b' = 0.45$ to $0.5\ \mathrm{GeV}/c$.

In Fig. 4.2 we compare the results of Eq. (4.5) integrated over y_2 with data taken from Darriulat [1]. In Fig. 4.3 we compare the results of Eq. (4.2) integrated over y_2 with data of Kephart et al. [18]. In Fig. 4.4 we compare same side and opposite side

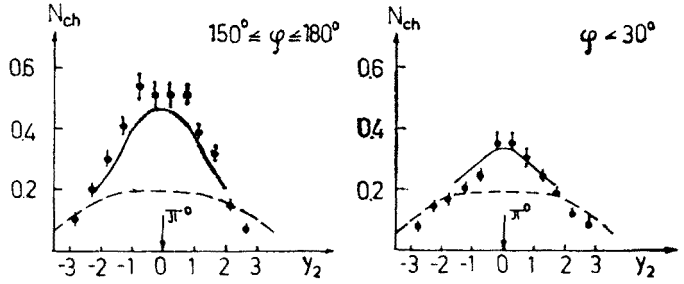

Fig. 4.4. The number of charged particles per event per 0.5 unit of rapidity per $\Delta\varphi = 60°$ as function of y_2 for trigger rapidity $y_1 = 0$ on the opposite side ($150° \leqslant \varphi \leqslant 180°$) and same side ($\varphi \leqslant 30°$) as compared with data of Ref. [19]. The theoretical curves were added to the background

associated multiplicities inside the azimuthal acceptance $\Delta\Phi = 30°$ as function of the rapidity. These distributions are calculated according to (4.2) and (4.5). We add the calculated associated multiplicities to the background given by the experimentalists. These curves we compare with data of the ACHM collaboration [19].

We find in these three Figures reasonable agreement between the data and our calculation. This agreement can be interpreted as evidence that the hard collision model describes also the associated multiplicities in their absolute size, $q_{\perp_1}$ and y_2 dependence consistently.

5. *Summary*

1. In Section 2 we have introduced a new parametrisation for jet fragmentation and uncorrelated approximation for jet production which permit an easy evaluation of the integral expressions defining inclusive distributions of large transverse momentum events in the case that the transverse momenta of particles relative to the jet axis are taken into account.

2. We calculate the distributions and correlations of two large $q_\perp$ particles at the same side and opposite side in the variable $\Delta y = y_1 - y_2$ and $\Delta y = y_2 - y_3$, resp. The agreement with recent data on same side and opposite side rapidity correlations can be interpreted as evidence for two jets in large $q_\perp$ reactions.

3. We work out expressions for large $q_\perp$ associated multiplicities in the hard collision model. The agreement with presently available data indicates that the absolute size, trigger transverse momentum and rapidity dependence of associated multiplicities can be consistently described within the framework of the hard collision model.

APPENDIX A

Inclusive two-particle distribution from jet fragmentation

Similar as in Sect. 2, we define the two-particle distribution from the fragmentation of *one* jet in the overall c.m.s.

$$\frac{d^6n(\hat{s})}{dq_{\perp 1}dq_{\perp 2}dy_1dy_2d\varphi_1d\varphi_2} = \frac{(F+1)^2}{q_{\perp 1}q_{\perp 2}}\mathscr{A}_2\left(\frac{\sqrt{\hat{s}}}{2}\right)\left(1-\frac{q_{\perp 1}+q_{\perp 2}}{P_\perp}\right)^F$$

$$\times \frac{1}{\pi c_1 c_2}\exp\left[-\frac{(y_1-Y_J)^2}{c_1^2}-\frac{(y_2-Y_J)^2}{c_2^2}\right]$$

$$\times \frac{1}{\pi c_1 c_2}\exp\left[-\frac{(\varphi_1-\Phi_J)^2}{c_1^2}-\frac{(\varphi_2-\Phi_J)^2}{c_2^2}\right]. \tag{A.1}$$

Here and in the following we abbreviate $c_i = b/q_{\perp i}$, $i = 1, 2, 3$. The normalisation $\mathscr{A}_2(\sqrt{\hat{s}}/2)$ is found through the transverse momentum sum rule

$$\int_0^{P_\perp - q_{\perp 1}} q_{\perp 2}dq_{\perp 2}\int dy_1 d\varphi_1 \frac{d^6n(\hat{s})}{dq_{\perp 1}dq_{\perp 2}dy_1dy_2d\varphi_1d\varphi_2} = (P_\perp - q_{\perp 1})\frac{dn(\hat{s})}{dq_{\perp 1}dy_1d\varphi_1}. \tag{A.2}$$

Asymptotically, $\mathscr{A}_2\left(\frac{\sqrt{\hat{s}}}{2}\right) \sim 1$.

The two-particle distribution integrated over the variables of particle 2 is obtained from the two-particle distribution (A.1)

$$\left\{\langle n_2(s)\rangle^*_{q_{\perp 1}}\frac{d^3n(\hat{s})}{dq_{\perp 1}dy_1d\varphi_1}\right\}$$

$$= \int_{\frac{b'}{\cosh \hat{Y}_J}}^{\frac{\hat{E}_J}{\cosh \hat{Y}_J} - q_{\perp 1}} dq_{\perp 2}\int_{Y_L(\hat{Y}_J,\vec{q}_1)}^{Y_U(\hat{Y}_J,\vec{q}_1)} dy_2 \int_{\Phi_L(\Phi_J,\vec{q}_1)}^{\Phi_U(\Phi_J,\vec{q}_1)} d\varphi_2 \frac{d^6n(\hat{s})}{dq_{\perp 1}dq_{\perp 2}dy_1dy_2d\varphi_1d\varphi_2}. \tag{A.3}$$

Approximating the proper kinematical limits of the y_2 integration by $Y_L \to -\infty$, $Y_o \to \infty$ and of the φ_2 integration by $\Phi_L \to -\infty$ and $\Phi_u \to \infty$, we obtain for $F = 1$ or 2 the following result

$$\left\{\langle n_2(\hat{s})\rangle_{q_1}^{*} \frac{d^3n(\hat{s})}{dq_{\perp 1}dy_1d\varphi_1}\right\} \sim \frac{1}{c_1\sqrt{\pi}} e^{-\frac{(y_1-Y_J)^2}{c_1^2}} \frac{1}{c_1\sqrt{\pi}} e^{-\frac{(\varphi_1-\Phi_J)^2}{c_1^2}}$$

$$\times \left[\left(1-\frac{q_{\perp 1}}{P_\perp}\right)^F \ln\left(\frac{\hat{E}_J\left(1-\frac{q_{\perp 1}}{P_\perp}\right)}{b'}\right) - F\left(1-\frac{q_{\perp 1}}{P_\perp}-\frac{b'}{\hat{E}_J}\right)\left(1-\frac{q_{\perp 1}}{P_\perp}\right)^{F-1}\right.$$

$$\left. + \frac{F-1}{2}\left(\left(1-\frac{q_{\perp 1}}{P_\perp}\right)^2 - \frac{b'^2}{\hat{E}_J^2}\right)\right],$$

where

$$\frac{b'}{\hat{E}_J} < \left(1-\frac{q_{\perp 1}}{P_\perp}\right). \tag{A.4}$$

The curly brackets above on the left side indicate that the expression in these brackets is *not* the product of a single particle distribution and the jet multiplicity.

APPENDIX B

Approximate expressions for inclusive distributions at large tranverse momentum

In this Appendix we give approximate expressions for inclusive distributions using the simple uncorrelated approximation for the two-jet production cross section (2.14) and the jet fragmentation functions (2.3) and (A.1). We put $\mathscr{A}_1(\sqrt{\hat{s}}/2) = \mathscr{A}_2(\sqrt{\hat{s}}/2) = 1$.

Inclusive single particle distribution

$$\frac{d\sigma}{dy_1dq_{\perp 1}d\varphi_1} = \int_{q_{\perp 1}}^{\sqrt{\hat{s}}/2} dP_\perp \int_{Y_{s1}}^{Y_{s2}} dY_s \int_{Y_{o1}}^{Y_{o2}} dY_o \int_{\varphi_1-\pi/2}^{\varphi_1+\pi/2} d\Phi \frac{d^4\sigma_J}{dY_sdY_odP_\perp d\Phi} \frac{d^3n(\hat{s})}{dq_{\perp 1}d\varphi_1dy_1}. \tag{B.1}$$

With our parametrisation for jet production and jet fragmentation the four integrals factorize. Extending the Y_s and Y_o integrations to the range $-\infty \leqslant Y_s, Y_o \leqslant +\infty$ we obtain

$$\frac{d\sigma}{dy_1dq_{\perp 1}d\varphi_1} = \operatorname{erf}\left(\frac{\pi}{2c_1}\right) W_1(y_1, B_s, c_1) \frac{CF!(N-2)!}{q_{\perp 1}^{N-2}(F+N-1)!} e^{-\frac{2Dq_{\perp 1}}{\sqrt{s}}}. \tag{B.2}$$

Here is

$$W_1(y_1, B_s, c_1) = \frac{1}{\sqrt{\pi}} \frac{1}{\sqrt{2B_s^2+c_1^2}} \exp\left(-\frac{y_1^2}{2B_s^2+c_1^2}\right) \tag{B.3}$$

and

$$c_i = \frac{b}{q_{\perp i}}. \tag{B.4}$$

Same side two-particle distribution

We give the expression integrated over $d(y_1+y_2)$ and integrated over the azimuthal angle φ_2 in the range $\varphi_1-\Delta\Phi \leqslant \varphi_2 \leqslant \varphi_1+\Delta\Phi$

$$\frac{d^4\sigma}{dq_{\perp 1}dq_{\perp 2}d(y_1-y_2)d\varphi_1} = \int_{\varphi_1-\Delta\Phi}^{\varphi_1+\Delta\Phi} d\varphi_2 \int_{-\infty}^{\infty} d(y_1+y_2) \int_{q_{\perp 1}+q_{\perp 2}}^{\sqrt{s}/2} dP_\perp$$

$$\times \int_{Y_{o1}}^{Y_{o2}} dY_o \int_{Y_{s1}}^{Y_{s2}} dY_s \int_{\varphi_{max}-\pi/2}^{\varphi_{min}+\pi/2} d\Phi \frac{d^4\sigma_J}{dY_s dY_o dP_\perp d\Phi} \frac{d^6n(\hat{s})}{dq_{\perp 1}dq_{\perp 2}dy_1dy_2d\varphi_1d\varphi_2}, \tag{B.5}$$

$$\varphi_{\substack{max\\(min)}} = \underset{(min)}{max}(\varphi_1, \varphi_2). \tag{B.6}$$

Proceeding as above we obtain

$$\frac{d^4\sigma}{dq_{\perp 1}dq_{\perp 2}d(y_1-y_2)d\varphi_1} = A_1(\Delta\Phi, c_1, c_2)W_2((y_1-y_2), B_s, c_1, c_2)$$

$$\times \frac{(F+1)^2}{q_{\perp 1}q_{\perp 2}} \frac{1}{(q_{\perp 1}+q_{\perp 2})^{N-1}} \exp\left(-\frac{2D(q_{\perp 1}+q_{\perp 2})}{\sqrt{s}}\right) \frac{CF!(N-2)!}{(F+N-1)!}. \tag{B.7}$$

Here we have abbreviated

$$W_2((y_1-y_2), B_s, c_1, c_2) = \frac{1}{\sqrt{\pi}\sqrt{\frac{c_1^2c_2^2}{2B_s^2}+c_1^2+c_2^2}} \exp\left[-\frac{(y_1-y_2)^2}{\frac{c_1^2c_2^2}{2B_s^2}+c_1^2+c_2^2}\right]. \tag{B.8}$$

The azimuthal acceptance is

$$A_1(\Delta\Phi, c_1, c_2) = \int_{-\Delta\Phi}^{+\Delta\Phi} d\varphi_2 \frac{1}{2\sqrt{\pi}} \frac{1}{\sqrt{c_1^2+c_2^2}} \exp\left[-\frac{\varphi_2^2}{c_1^2+c_2^2}\right]$$

$$\times \left\{\operatorname{erf}\left[\frac{\pi}{2}\sqrt{\frac{1}{c_1^2}+\frac{1}{c_2^2}} - \frac{\varphi_2}{c_2^2\sqrt{\frac{1}{c_1^2}+\frac{1}{c_2^2}}}\right]\right.$$

$$\left. -\operatorname{erf}\left[\left(\varphi_2-\frac{\pi}{2}\right)\sqrt{\frac{1}{c_1^2}+\frac{1}{c_2^2}} - \frac{\varphi_2}{c_2^2\sqrt{\frac{1}{c_1^2}+\frac{1}{c_2^2}}}\right]\right\}. \tag{B.9}$$

For sufficiently large $\Delta\Phi$ and sufficiently large transverse momenta $q_{\perp 1}$ and $q_{\perp 2}$,

$$A_1(\Delta\Phi, c_1, c_2) \simeq 1. \tag{B.10}$$

Distribution for one trigger particle and one particle on the opposite side

We give this expression integrated over the azimuthal angle φ_2 in the range $\varphi_1+\pi-\Delta\Phi \leqslant \varphi_2 \leqslant \varphi_1+\pi+\Delta\Phi$

$$\frac{d^5\sigma}{dq_{\perp 1}dq_{\perp 2}d\varphi_1 dy_1 dy_2} = \int_{\varphi_1+\pi-\Delta\Phi}^{\varphi_1+\pi+\Delta\Phi} d\varphi_2 \int_{q_{\perp 1}}^{\sqrt{s}/2} dP_\perp \int_{Y_{o1}}^{Y_{o2}} dY_o \int_{Y_{s1}}^{Y_{s2}} dY_s \int_{\varphi_{\max}-\pi/2}^{\varphi_{\min}+\pi/2} d\Phi$$

$$\times \frac{d^4\sigma_J}{dY_s dY_o dP_\perp d\Phi} \frac{d^3n_s(\hat{s})}{dq_{\perp 1}dy_1 d\varphi_1} \frac{d^3n_o(\hat{s})}{dq_{\perp 2}dy_2 d\varphi_2} \tag{B.11}$$

with

$$\varphi_{\substack{\max \\ (\min)}} = \underset{(\min)}{\max}(\varphi_1+\pi, \varphi_2). \tag{B.12}$$

As above we obtain

$$\frac{d^5\sigma}{dq_{\perp 1}dq_{\perp 2}dy_1 dy_2 d\varphi_1} = A_1(\Delta\Phi, c_1, c_2) \cdot W_1(y_1, B_s, c_1)$$

$$\times W_1(y_2, B_o, c_2) \frac{C(F+1)^2}{q_{\perp 1}q_{\perp 2}} \int_{q_{\perp 1}}^{\sqrt{s}/2} dP_\perp \frac{1}{P_\perp^N} \exp\left(-\frac{2DP_\perp}{\sqrt{s}}\right)\left(1-\frac{q_{\perp 1}}{P_\perp}\right)^F\left(1-\frac{q_{\perp 2}}{P_\perp}\right)^F. \tag{B.13}$$

Distribution for the trigger particle and two-particles on the opposite side

We give the expression integrated over $d(y_2+y_3)$ and integrated over the azimuthal angles φ_2 and φ_3 in the interval $\varphi_1+\pi-\Delta\Phi \leqslant \varphi_i \leqslant \varphi_1+\pi+\Delta\Phi$, $i = 2, 3$.

$$\frac{d^6\sigma}{dq_{\perp 1}dq_{\perp 2}dq_{\perp 3}dy_1 d(y_2-y_3)d\varphi_1} = A_2(\Delta\Phi, c_1, c_2, c_3)$$

$$\times W_1(y_1, B_s, c_1) W_2((y_2-y_3), B_o, c_2, c_3)$$

$$\times \frac{C(F+1)^3}{q_{\perp 1}q_{\perp 2}q_{\perp 3}} \int_{q_{\perp 1}}^{\sqrt{s}/2} dP_\perp \frac{1}{P_\perp} \exp\left(-\frac{2DP_\perp}{\sqrt{s}}\right)\left(1-\frac{q_{\perp 1}}{P_\perp}\right)^F\left(1-\frac{q_{\perp 2}+q_{\perp 3}}{P_\perp}\right)^F. \tag{B.14}$$

The azimuthal acceptance is expressed by the function

$$A_2(\Delta\Phi, c_1, c_2, c_3) = \frac{1}{\pi\sqrt{c_1^2c_2^2+c_1^2c_3^2+c_2^2c_3^2}} \int_{-\Delta\Phi}^{\Delta\Phi} d\varphi_2 \int_{-\Delta\Phi}^{\Delta\Phi} d\varphi_3$$

$$\times \exp\left[-\frac{c_3^2\varphi_2^2+c_2^2\varphi_3^2+c_1^2(\varphi_2-\varphi_3)^2}{c_1^2c_2^2+c_1^2c_3^2+c_2^2c_3^2}\right] \tfrac{1}{2}\left\{\operatorname{erf}\left[\left(\varphi_{\max}-\frac{\pi}{2}\right)\sqrt{\frac{1}{c_1^2}+\frac{1}{c_2^2}+\frac{1}{c_3^2}}\right.\right.$$

$$\left.\left.-\frac{\frac{\varphi_2}{c_2^2}+\frac{\varphi_3}{c_3^2}}{\sqrt{\frac{1}{c_1^2}+\frac{1}{c_2^2}+\frac{1}{c_3^2}}}\right]-\operatorname{erf}\left[\left(\varphi_{\min}+\frac{\pi}{2}\right)\sqrt{\frac{1}{c_1^2}+\frac{1}{c_2^2}+\frac{1}{c_3^2}}-\frac{\frac{\varphi_2}{c_2^2}+\frac{\varphi_3}{c_3^2}}{\sqrt{\frac{1}{c_1^2}+\frac{1}{c_2^2}+\frac{1}{c_3^2}}}\right]\right\}. \qquad \text{(B.15)}$$

REFERENCES

[1] P. Darriulat, Rapporteur talk, Proc. XVIII Int. Conf. on High Energy Physics, Tbilisi, Juli 1976, p. A4–23

[2] M. Della Negra, Rapporteur talk, Proc. VII Int. Conf. on Multi Particle Production, BRD, June 1976, p. 189.

[3] J. D. Bjorken, *Phys. Rev.* **D8**, 4098 (1973).

[4] G. Ranft, J. Ranft, *Nucl. Phys.* **B110**, 493 (1976), (quoted as I); J. D. Bjorken, Lecture in SLAC Summer Institute, 1975.

[6] S. D. Ellis, M. Jacob, P. V. Landshoff, *Nucl. Phys.* **B108**, 93 (1976).

[7] W. Furmański, J. Wosiek, Cracow preprint TPJU 7/76.

[8] J. Gasser, U. P. Sukhatme, Cambridge preprint, DAMPT 76–3.

[9] G. Preparata, G. Rossi, *Nucl. Phys.* **B111**, 111 (1976).

[10] J. Ranft, G. Ranft, *Acta Phys. Pol.* **B8**, 179 (1977), (quoted as II).

[11] J. Kripfganz, J. Ranft, CERN-preprint.

[12] P. Darriulat et al., *Nucl. Phys.* **B107**, 429 (1976).

[13] M. Della Negra, CERN-preprint, June 11, 1976 contribution the XVIII Int. Conf. on High Energy Physics, Tbilisi 1976.

[14] S. D. Ellis, M. Kislinger, *Phys. Rev.* **D9**, 2027 (1974).

[15] M. Della Negra et al., CERN-preprint, June 21, 1976 submitted to the XVIII Int. Conf. on High Energy Physics, 1976.

[16] J. Abad, A. Cruz, J. L. Alonso, *Nucl. Phys.* **B115**, 533 (1976).

[17] V. Barger, R. J. N. Phillips, *Nucl. Phys.* **B73**, 269 (1974).

[18] R. Kephart et al., *Phys. Rev.* **D14**, 2909 (1976).

[19] K. Eggert et al., *Nucl. Phys.* **B98**, 73 (1975).